

Production of neutrons and spallation products by high-energy particle beams

Takashi Nakamura

Prof. Emeritus of Tohoku Univ.

Adviser of Shimizu Corporation

Presentation at SATIF-10

CERN, Geneva, June 2, 2010

Contents

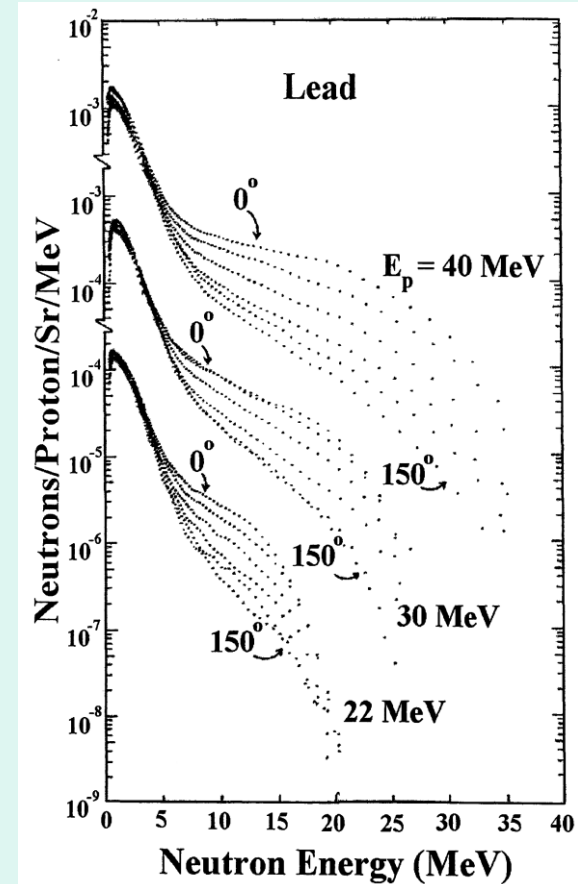
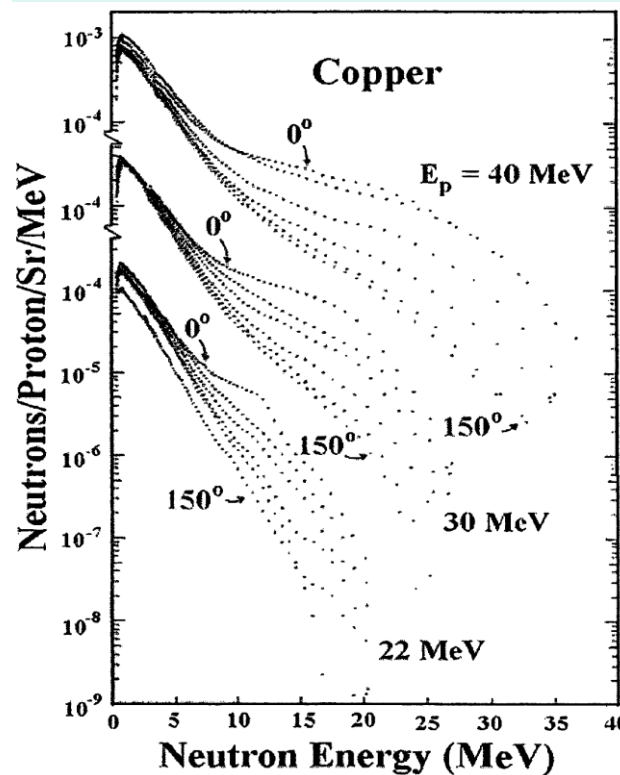
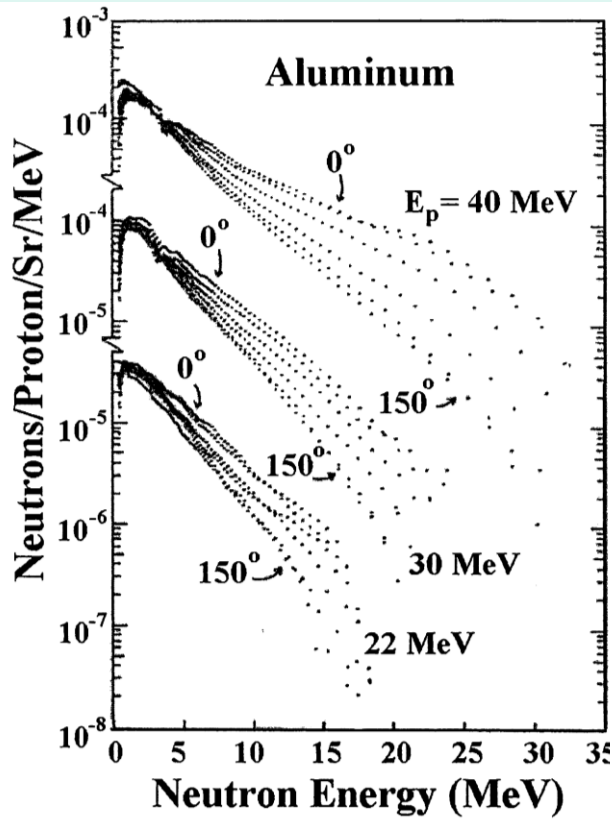
- This review summarizes experimental results up to 2008 year on energy and angular distribution of neutrons produced from thick targets of various materials bombarded by protons, deuterons, He and heavier ions having wide energy range from MeV to GeV. Total neutron yields are also presented.
- Production cross section data for spallation by proton to Ar ion are also summarized, as well as excitation functions, mass-yield distributions, and induced activities.

1. Thick target yield (TTY) means the angular-energy distribution of secondary particles, especially neutrons produced from a thick target which has enough thickness to fully stop the incident particles. The TTY data are indispensable for estimating source terms used in the accelerator shielding design. A number of experiments to give the TTY data have ever been published. In this presentation, some typical works are picked up for p, d, He-3 and He-4 projectiles, then C and Fe ions.
2. Spallation products production cross section are the basic data for induced activity estimation in accelerator facilities. Here the experimental data are presented for heavy ion induced products and activities.

Proj.	Energy (MeV)	Target	Emission Angle (degree)	Facility	Neutron Detection	Ref.
p	15	Li-7	0-45		NE218, TOF	3
	15, 18, 23	Li, Be	0 (0-40)		Stilben, TOF	4
	22, 30, 40	C, Al, Cu, Ta, Ag, Pb	0 - 150	NSCL	NE213, TOF	5
	25,35,45,5 5	Be	0-50	UC Davis	NE213, TOF	6
	30	C-13	0 - 120	Jyvaskira	Position Sensitive Detector, TOF	7
	30	C, Fe, Cu, Pb	0-135	INS	NE213, Unfolding	8
	35, 46	Be	0, 15, 45		NE213, TOF	9
	35, 50, 70	Fe, Cu	0, 30, 60, 90, 110	CYRIC	NE213, TOF	10
	40	Al, Fe, Cu, Ta, SUS	0, 45, 90	Milano	Activation	11
	50	C, Al, Ta, W	0 - 90	CYRIC	NE213, TOF	12
	52	C, Fe, Cu, Pb	0-75	INS	NE213, Unfolding	13
	68	Be, C, Al, Cu, Au	0, 30, 60, 120	TIARA	NE213, TOF	14
	72	Cu	90-150	SIN(PSI)	Activation	15
	90	C-13	0 - 150		NE213, TOF	16
	113	Be, C, Al, Fe, U	7.5- 150	LAMPF	BC418, TOF	17
	140	C, Al, Fe, Pb	0, 90, 180	RCNP	NE213, TOF	18
	210	Fe	0-110	RIKEN	NE213, TOF	19
	250, 350	C, Al, Fe, Pb	0	RCNP	NE213, TOF	20
	256	C, Al, Fe, U	30-150	LAMPF	BC418, TOF	21
	500, 1500	Pb	15- 150	KEK	NE213, TOF	22
	500, 1500	W	15- 150	KEK	NE213, TOF	23
	590	Pb, U, Pb-Bi	30, 90, 150	SIN(PSI)	NE102, NE228, TOF	24
	660	Pb	60	JINR	NaI(Tl), TOF	25
	740	dep U + Steel	50, 130	LBL	NE102, NE228, TOF	26
	740	U	50, 130	LAMPF	NE213, Unfolding	27
	800, 1200,	Pb Fe W Al	0 - 160	SATURN	NE213, TOF	28

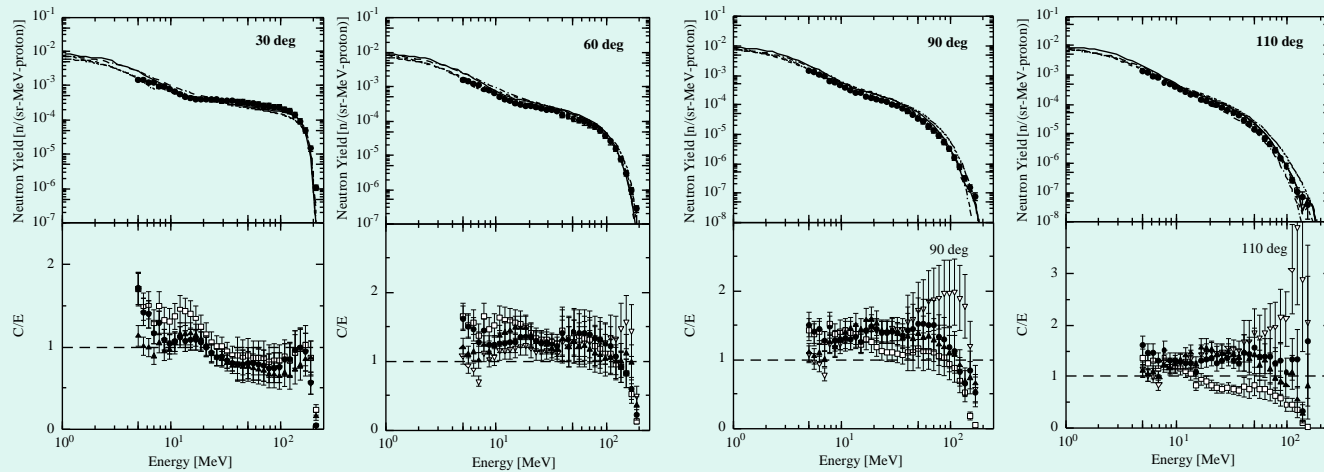
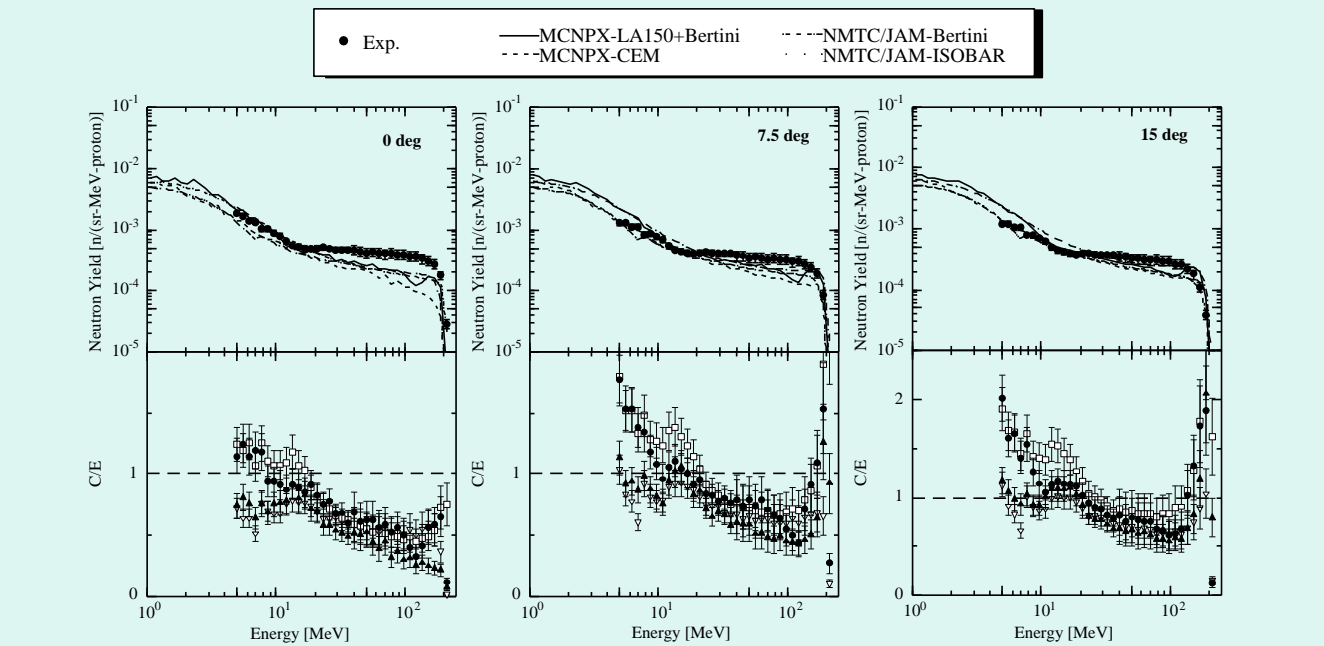
Proj.	Energy (MeV)	Target	Emission Angle (degree)	Facility	Neutron Detection	Ref.
d	8,12,15	Li-7	0 - 45		NE218, TOF	3
	15, 18 23	Li, Be	0 (0-40)		Stilben, TOF	4
	16, 28	Be	0, 15, 45		NE102A, TOF	9
	16, 33, 50	Be, C, Mo, Cu, Ta, Au	0 - 64		NE111, TOF	42
	17, 20, 28	Be, C, U	0 - 20	IPN Orsay	NE213, TOF	43
	25	Li, Be	0 - 90	CYRIC	NE213, TOF	44
	33	C, Fe, Cu, Pb	0 - 135	INS	NE213, Unfolding	45
	40	Li	0 - 110	CYRIC	NE213, TOF	46
	40	C, Al	0 - 110	CYRIC	NE213, TOF	47
	40	Be	0 - 90	ORNL	NE213, TOF	48
	80, 160	Be, C	2.3 - 33.3		NE213, TOF	49
	200	Be, U	0 - 84	Saturne	Activation	50

Proj.	Energy (MeV)	Target	Emission Angle (degree)	Facility	Neutron Detection	Ref.
^3He	44	Be	0, 15, 45		NE102A, TOF	9
	65	C, Fe, Cu, Pb	0 - 135	INS	NE213, Unfolding	45
α	30, 40 50	Al, Ti	0, 30, 45	VECC	NE213, Unfolding	52
	40, 50, 60	Be, Ta, Au	0, 30, 60, 90	VECC	NE213, Unfolding	53
	65	C, Fe, Cu, Pb	0 - 135	INS	NE213, Unfolding	45
	80	Ta	0, 60, 90	LBL	Activation	54
	100	C, Fe, Zr, Au	0 - 120	TIARA	NE213, TOF	15
$^6\text{Li}, ^7\text{Li}$	40	^7Li , Be, C, Cu	0 - 120	Geel	NE213, TOF	55
^{11}B	42, 62	Al	0, 90	BARC-TIFR	BC501, TOF	56
^{12}C	54, 65, 75, 84	Al	0, 90	BARC-TIFR	BC501, TOF	56
	220	C, Fe, Zr, Au	0 - 120	TIARA	NE213, TOF	57
Ar	95/nucleo n	C	0, 20, 45, 90	Saturne	Activation	50
	460	C, Fe, Zr, Au	0 - 120	TIARA	NE213, TOF	57

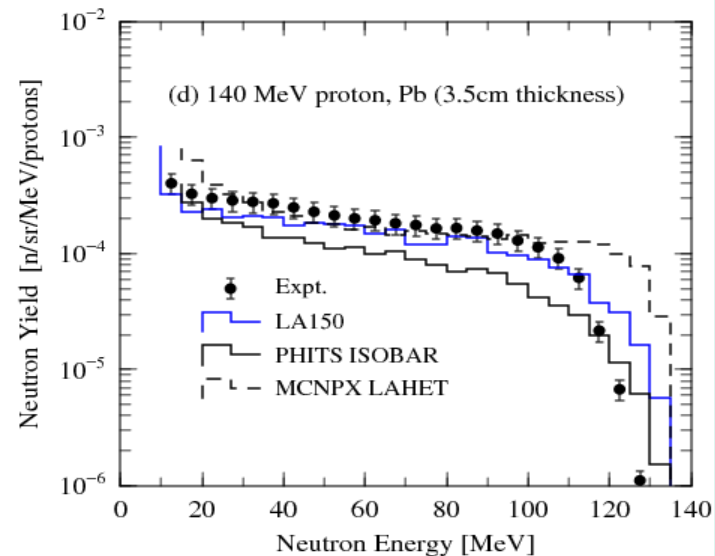
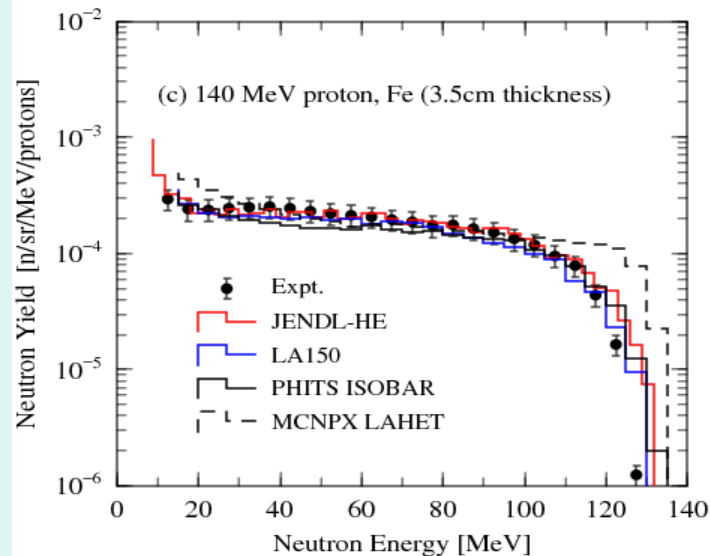
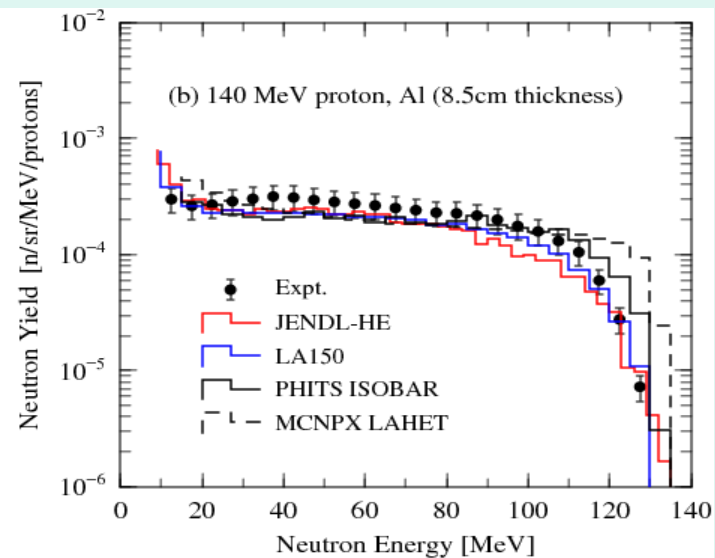
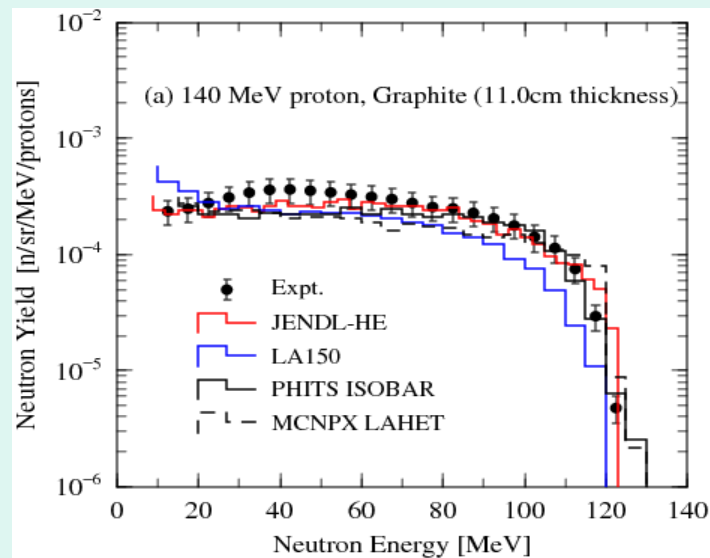


Neutron yield spectra from stopping Al, Cu and Pb targets bombarded by protons at energies of 22, 30 and 40 MeV. Each energy group has spectra at 0, 30, 60, 90, 120, and 150 degrees. Between the spectra labeled 0 and 150 degree are the other four spectra in monotonically descending order. (Amos et al. at NSCL, N.S.E. in 2004)

Two components can be seen: one below about 10 MeV, especially for heavier target coming from evaporation process and other above it from preequilibrium/cascade process.

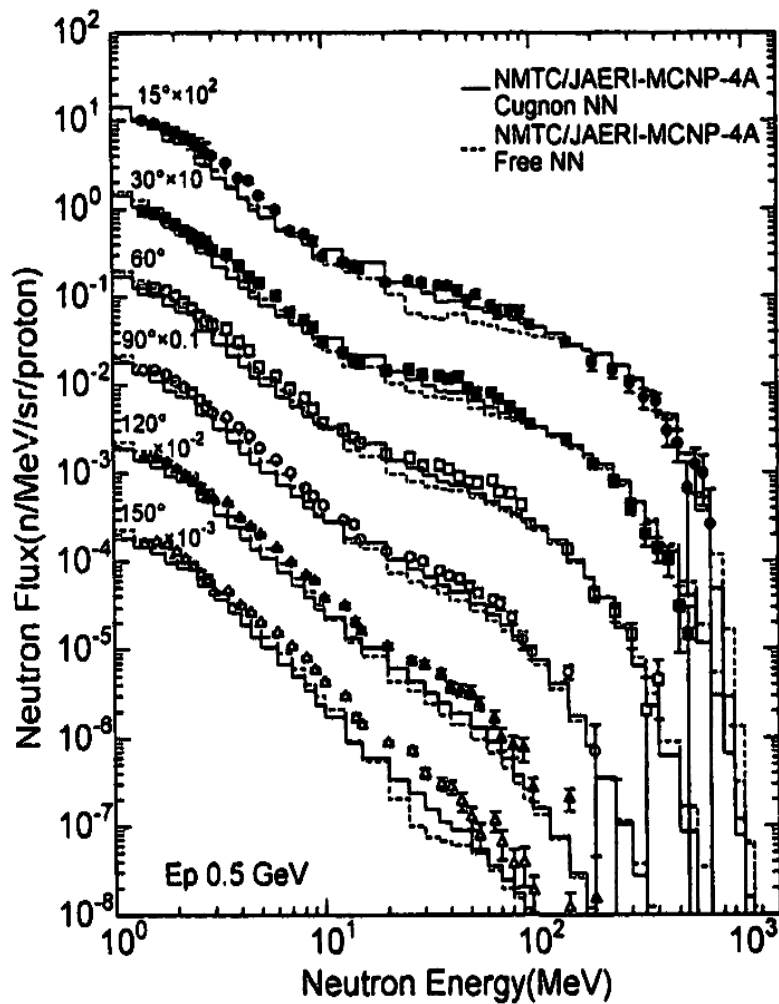


Neutron energy spectra from the iron target bombarded by 210 MeV proton compared with the calculations at angles of 0, 7.5, 15, 30, 60, 90 and 110 degrees. (Yonai et al. at RIKEN, NIM A in 2003)

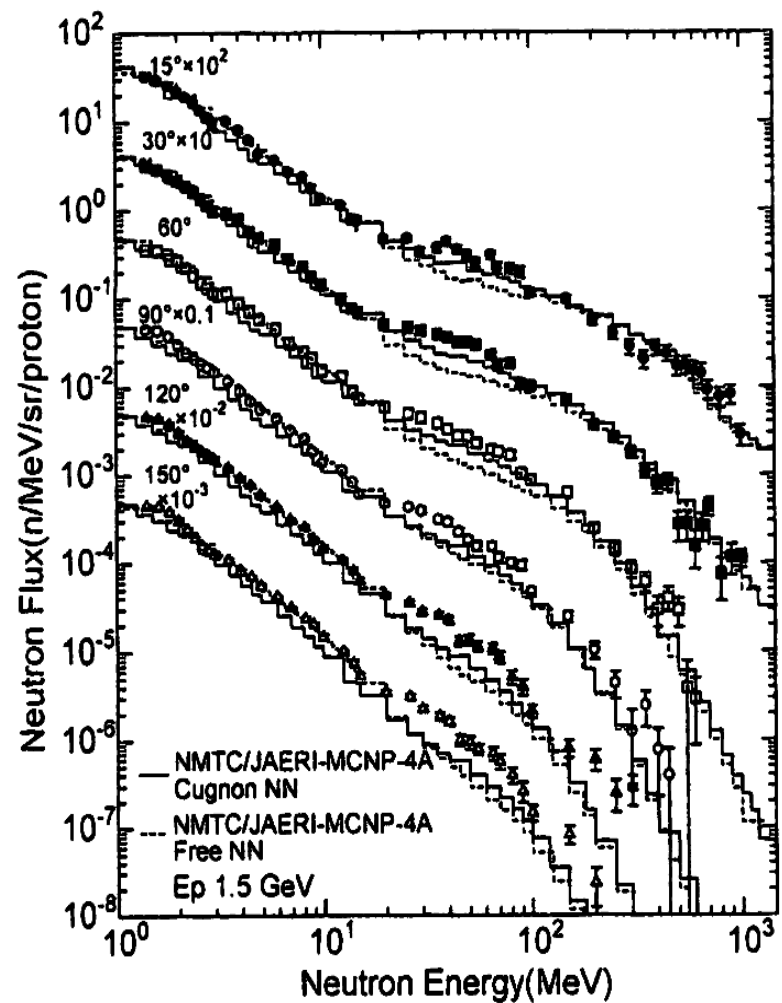


Neutron energy spectra for 140 MeV proton incidence at 0 degree on thick C, Al, Fe and Pb targets. The experimental results are compared with the calculated results with PHITS and MCNPX using data libraries, LA150 and JENDL-HE, reaction models, ISOBAR and LAHET (Iwamoto et al. at RCNP, Osaka-U., Nucl. Technol. In 2009)

(b)(b)

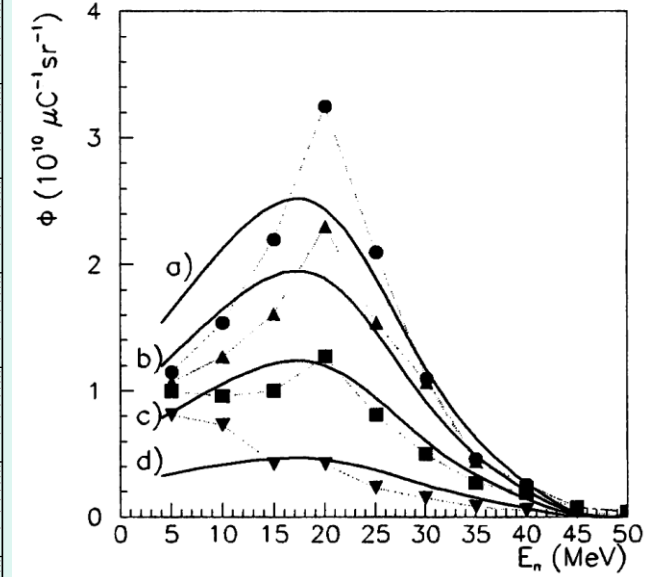
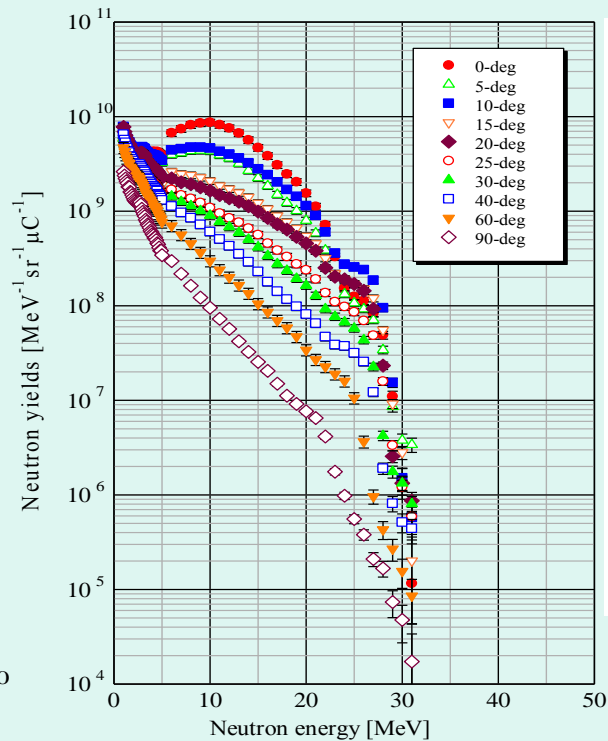
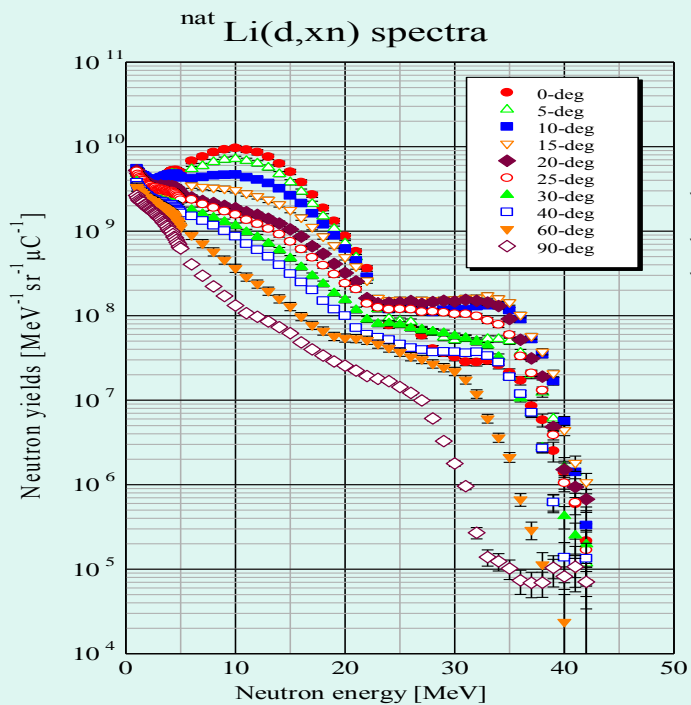


(a)



(b)

Neutron spectra for (a) 0.5 GeV and (b) 1.5 GeV protons incidence on thick lead target. Symbols stand for the experimental results. Dash and solid lines show results calculated with NMTC/JAERI and MCNP-4A using free nucleon-nucleon cross section (NNCS) and in-medium NNCS, respectively. (Meigo et al. at KEK, NIM A in 1999)

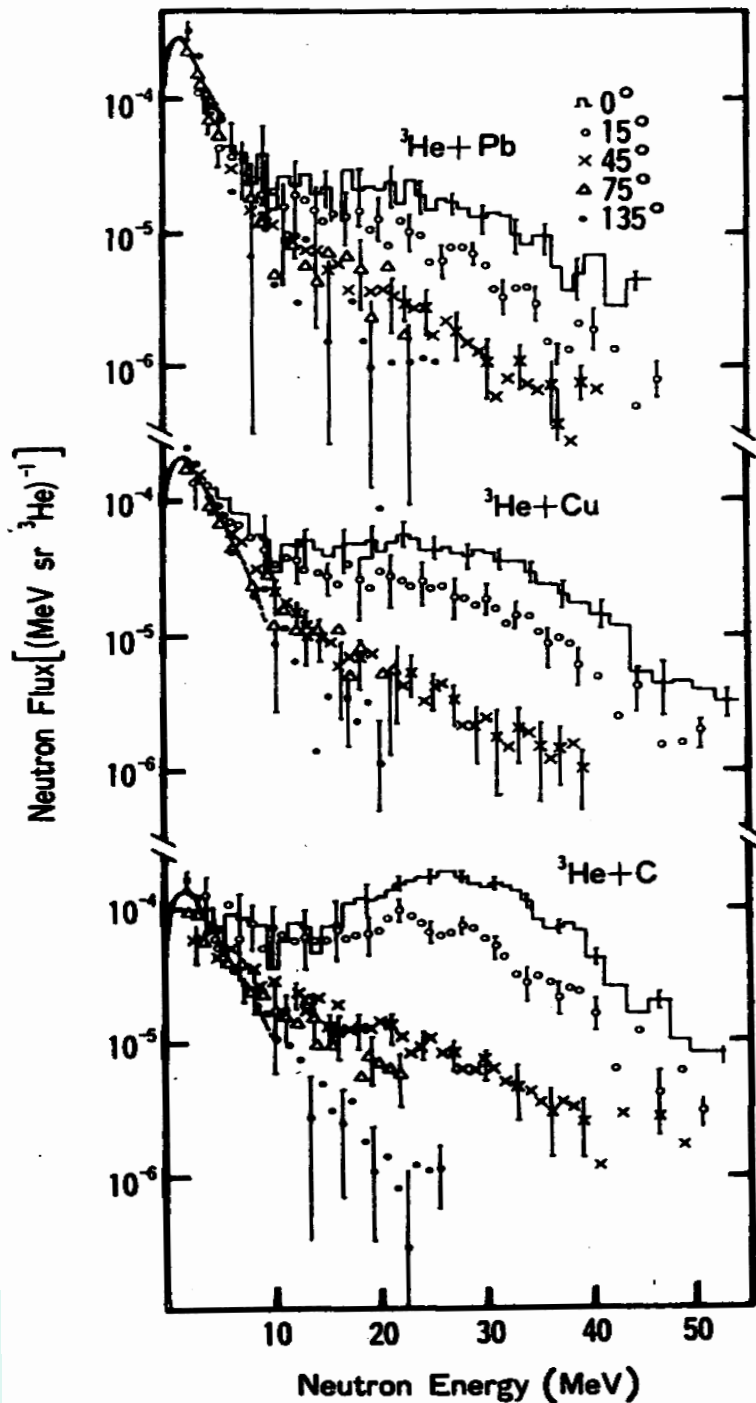


Li(d,n) spectra for 25 MeV deuteron
Q value of 15.7 MeV

Be(d,n) spectra for 25
MeV deuteron

Be(d,n) spectra at a) 0, b)
5, c) 10, d) 25 degrees
for 50MeV deuteron
compared with Serber
model
(Meulders et al. at
Louvain, PMB in 1975)

Neutron spectra of Li and Be targets for 25 and 50 MeV d. In addition to two components of evaporation and pre-equilibrium processes, a broad peak due to the stripping/breakup reaction of deuteron can be seen at about 40% energy of the incident deuteron energy. (Aoki et al. at CYRIC, Tohoku-U., JNST in 2004)



Neutron spectra of carbon, copper, and lead targets for 65-MeV ${}^3\text{He}$ injection at emission angles of 0, 15, 45, 75, and 135 deg. The solid curves indicate the Maxwellian distribution fitted to the neutron spectra.

The spectra have also two components of evaporation and pre-equilibrium/cascade processes, but in the forward direction, a broad peak of the breakup reaction of ${}^3\text{He}$ nuclei, (${}^3\text{He}, n2p$) can be seen.

(Shin et al. at INS, U-Tokyo, P. R. C in 1984)

Moving-source model of thick-target neutron yield

The moving source parameterization has been used successfully in reproducing inclusive charged particle and neutron spectra from charged particle interactions. The moving source model assumes there are three thermal moving sources:

- 1) One projectile-like source moving at a velocity near the incoming beam velocity,
- 2) A second target-like source moving very slowly in the laboratory frame
- 3) A third overlap source moving 1/2 to 1/3 of the velocity of the beam.

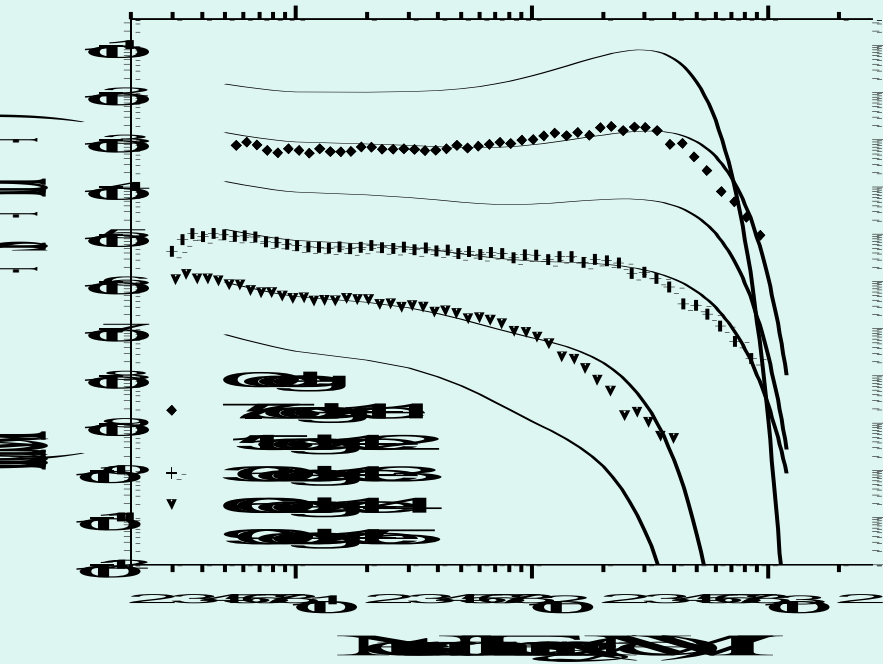
Each source is assumed to thermally emit nucleons with an isotropic distribution in its own frame.

The spectrum of nucleons in the source's rest frame has the Maxwellian form of $E^{1/2} \exp(-E/T)$,

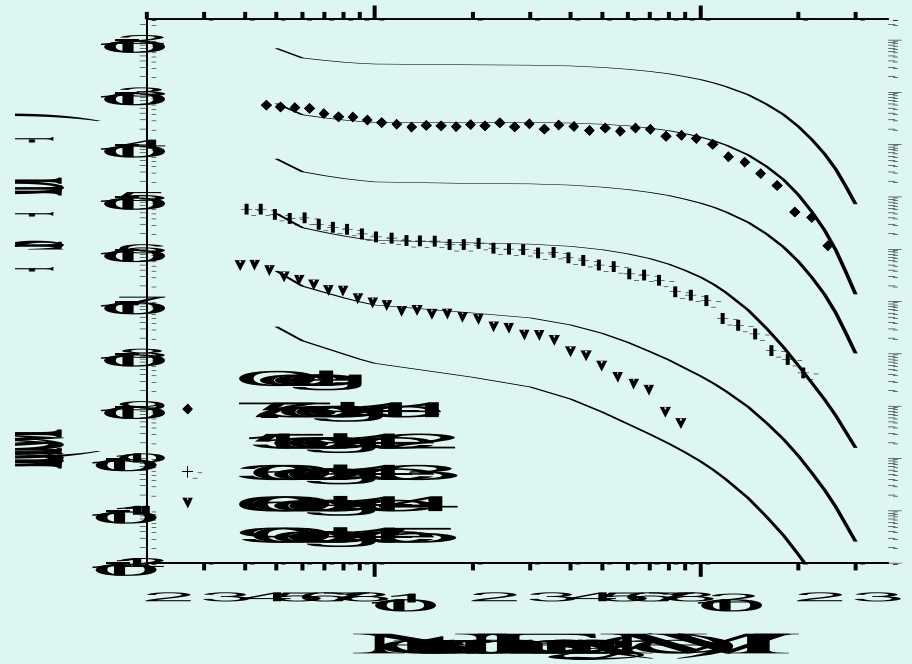
where E is the energy of the nucleon and T is the temperature of the source.

In the laboratory system, the complete distribution with respect to energy and angle is given in three terms of Maxwellian forms.

This formula is extended to apply the thick target neutron yield as shown in the next slide.



(a) 100 MeV/nucleon He stopping in Cu



(b) 400 MeV/nucleon C stopping in Cu

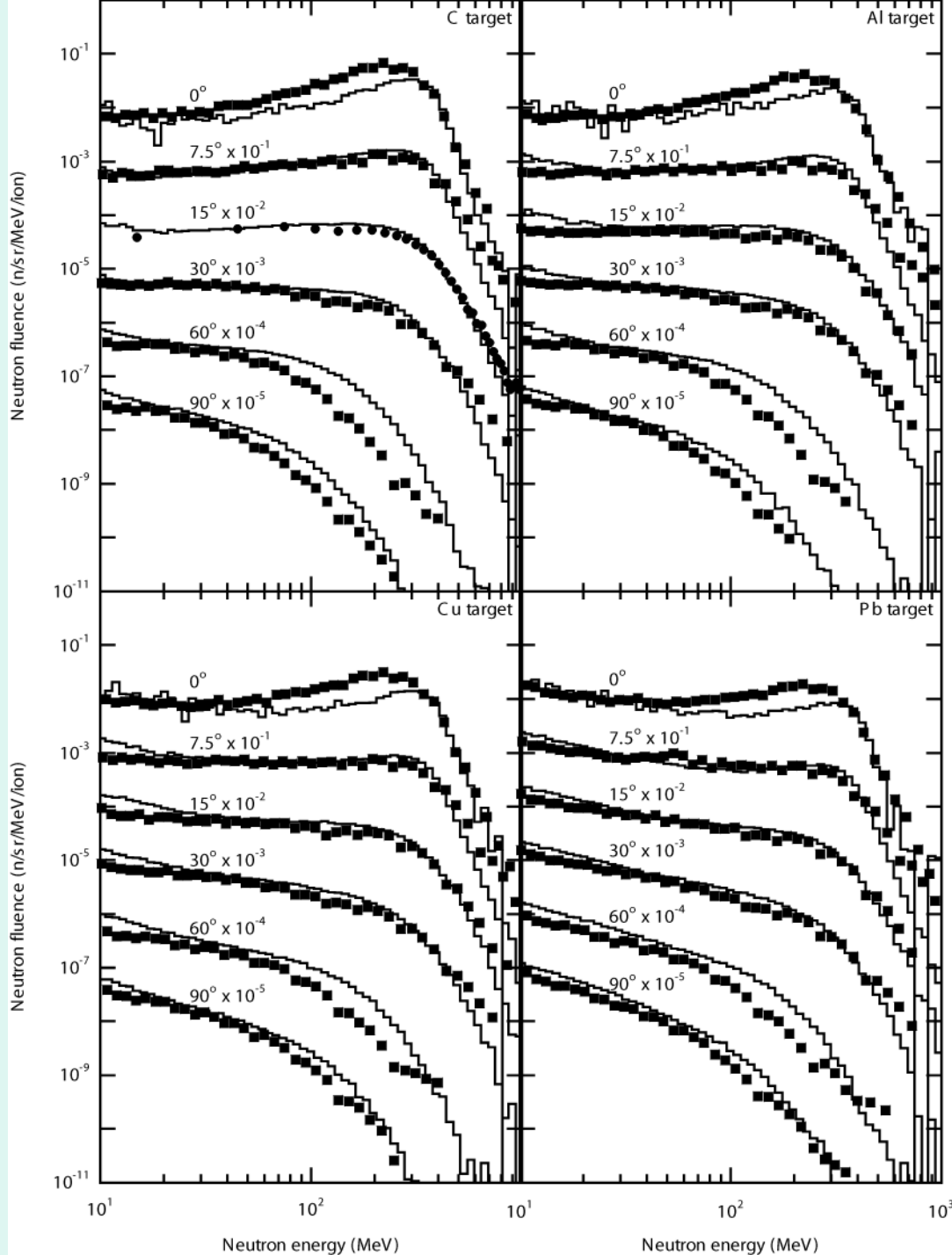
Moving source fits are shown in solid lines. Note the spectra are offset by the indicated factors of ten. (Kurosawa et al. at HIMAC, P. R. C in 2000)

Moving source model is given as

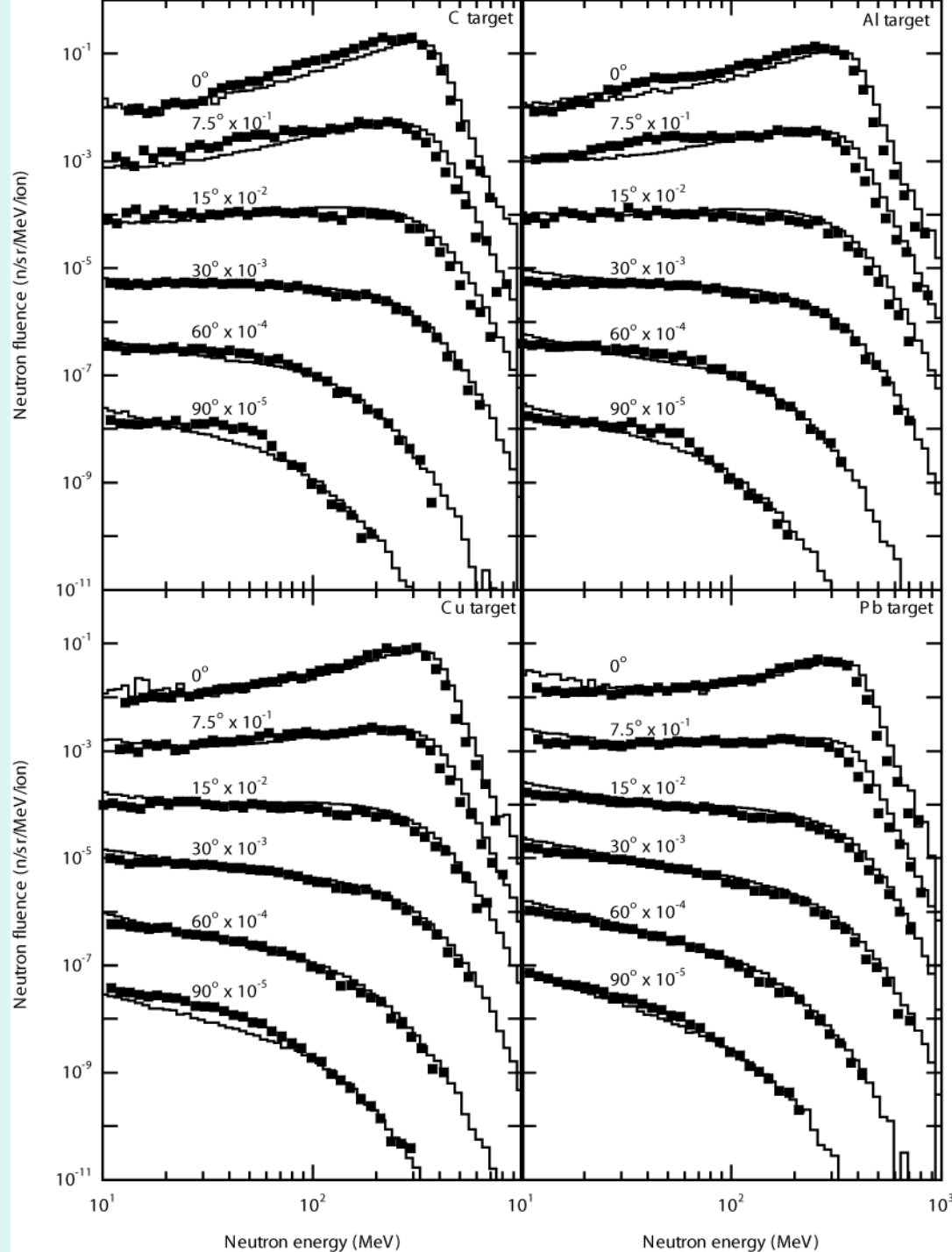
$$\frac{d^2Y}{dEd\Omega} = \left\{ \frac{N_0}{\sqrt{2\pi\sigma_c(\theta)^2}} \exp\left(-\frac{(E_n - E_c(\theta))^2}{2\sigma_c(\theta)^2}\right) \right\} + \left\{ \sum_{i=1}^2 N_i \frac{\sqrt{E_n}}{2(\pi T_i)^{3/2}} \exp\left(-\frac{E_s}{T_i}\right) \right\},$$

$$E_s = E_n + \varepsilon_i - 2\sqrt{\varepsilon_i E_n} \cos \theta.$$

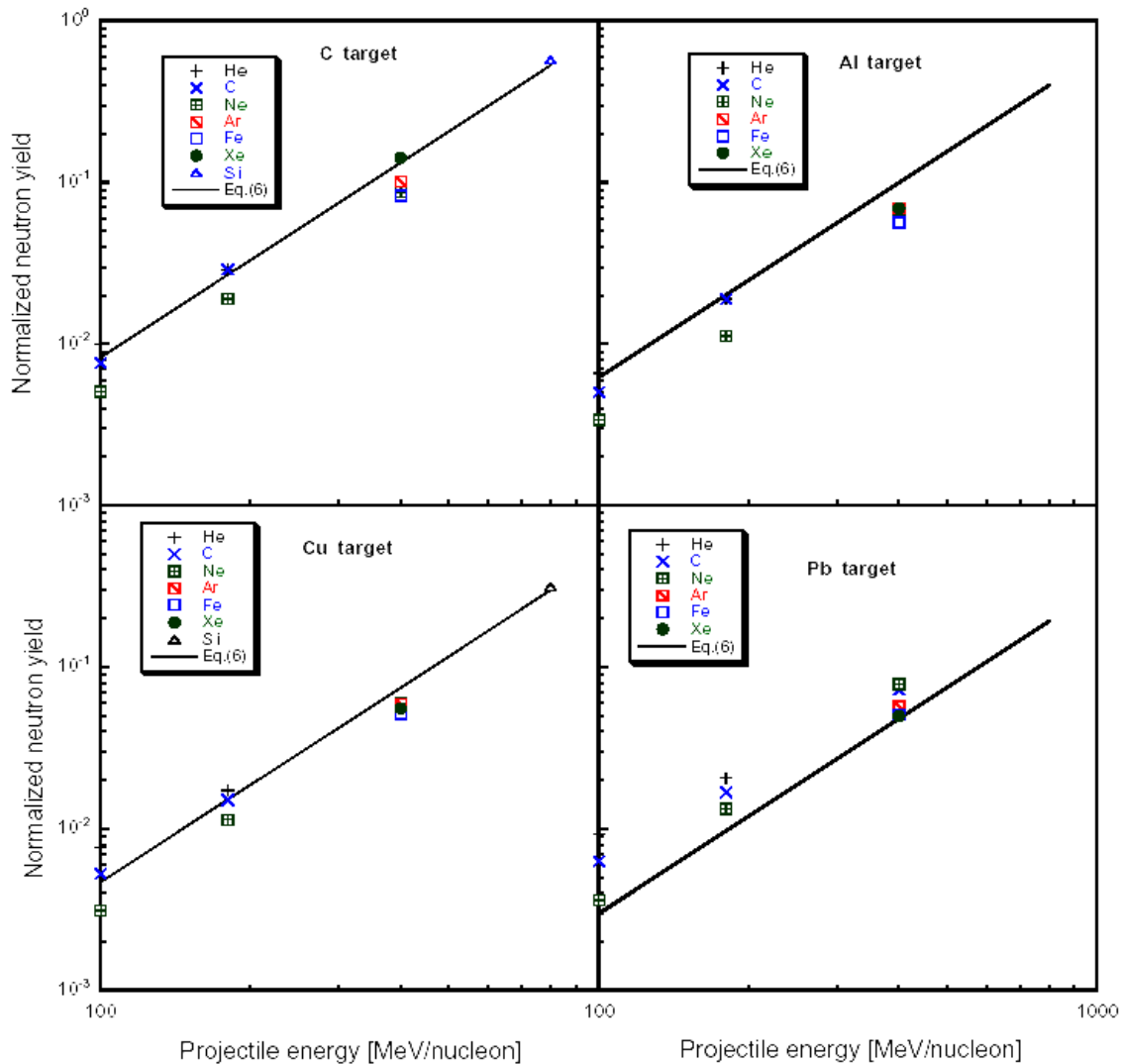
Beam ion and energy (MeV/nucleon)	Targets (cm)	Measured spectra	θ (deg)	Emin (MeV)	Facility
He (100)	C (5.0), Al (4.0), Cu (1.5), Pb (1.5)	TTY, n/d Ω , total	0, 7.5, 15, 30, 60, 90	5.5, 5, 4, 3.5, 3.5, 3	HIMAC [7,8]
He (155)	Al (8.26)	TTY, n/d Ω , total	10, 30, 45, 60, 90, 125, 160	10, 3, 3, 7, 4, 3, 3	NSCL [12]
He (160)	Pb (3.937)	TTY, Total	0, 45, 90, 120, 150	10, 3, 13, 13, 13	SREL [13]
He (177.5)	C (14.73), H ₂ O (22.86), Steel (4.445), Pb (3.937)	TTY, Total	0, 6, 15, 30, 45, 60, 90, 120, 135, 150	3, 10, 11, 11, 3, 10, 3, 13, 3, 13	SREL [13]
He (180)	C (16.0), Al (12.0), Cu (4.5), Pb (5.0)	TTY, n/d Ω , total	0, 7.5, 15, 30, 60, 90	17, 11, 5.5, 6.5, 3.5, 3.5	HIMAC [7,8]
C (100)	C (2.0), Al (1.0), Cu (0.5), Pb (0.5)	TTY, n/d Ω , total	0, 7.5, 15, 30, 60, 90	4, 4, 3.5, 3.5, 3, 3	HIMAC [7,8]
C (155)	Al (8.26)	TTY, n/d Ω , total	10, 30, 45, 60, 90, 125, 160	10, 3, 3, 7, 4, 3, 3	NSCL [12]
C (180)	C (6.0), Al (4.0), Cu (1.5), Pb (1.5)	TTY, n/d Ω , total	0, 7.5, 15, 30, 60, 90	5.5, 5.5, 3.5, 2.5, 3, 2.5	HIMAC [7,8]
C (400)	C (20.0), Al (15.0), Cu (5.0), Pb (5.0)	TTY, n/d Ω , total	0, 7.5, 15, 30, 60, 90	8.5, 5, 3.5, 3, 3, 3	HIMAC [7,8]
Ne (100)	C (1.0), Al (1.0), Cu (0.5), Pb (0.5)	TTY, n/d Ω , total	0, 7.5, 15, 30, 60, 90	6, 6, 5, 5.5, 5.5, 5	HIMAC [9]
Ne (180)	C (4.0), Al (3.0), Cu (1.0), Pb (1.0)	TTY, n/d Ω , total	0, 7.5, 15, 30, 60, 90	9, 6, 3.5, 3.5, 3, 3	HIMAC [9]
Ne (400)	C (11.0), Al (9.0), Cu (3.0), Pb (3.0)	TTY, n/d Ω , total	0, 7.5, 15, 30, 60, 90	6, 5.5, 4, 3, 3, 3	HIMAC [9]
Si (800)	C (23.0), Cu (6.5)	TTY, n/d Ω , total	0, 7.5, 15, 30, 60, 90	11, 8, 8, 4, 3.5, 3.5	HIMAC [10]
Ar (400)	C (7.0), Al (5.5), Cu (2.0), Pb (2.0)	TTY, n/d Ω , total	0, 7.5, 15, 30, 60, 90	10, 7, 3.5, 3.5, 3, 3	HIMAC [10]
Fe (400)	C (6.0), Al (4.0), Cu (1.5), Pb (1.5)	TTY, n/d Ω , total	0, 7.5, 15, 30, 60, 90, 120, 160	12, 11, 7, 4, 3, 3	HIMAC [10]
Nb (272)	Nb (1.0), Al (1.27)	TTY, n/d Ω , n/dE total	3, 6, 9, 12, 16, 20, 24, 28, 32, 36, 40, 48, 56, 64, 72, 80	20 (all angles)	Bevalac [11]
Nb (435)	Nb (0.51)	TTY, n/d Ω , n/dE total	3, 6, 9, 12, 16, 20, 24, 28, 32, 36, 40, 48, 56, 64, 72, 80	20 (all angles)	Bevalac [11]
Xe (400)	C (3.0), Al (2.0), Cu (1.0), Pb (1.0)	TTY, n/d Ω , total	0, 7.5, 15, 30, 60, 90	10, 6, 5, 3.5, 3.5, 3.5	HIMAC [10]
U-238 (1000)	Fe (20)	TTY, n/d Ω	0 – 20	50	GSI [6]



Neutron energy spectra for 400 MeV/nucleon C ion bombardment on thick C, Al, Cu and Pb targets. Marks indicate the experimental data and solid lines indicate the PHITS calculation. (Sato et al. at HIMAC, NIM A in 2007)



Neutron energy spectra for 400 MeV/nucleon Fe ion bombardment on thick C, Al, Cu and Pb targets. Marks indicate the experimental data and solid lines indicate the PHITS calculation. (Sato et al. at HIMAC, NIM A in 2007)



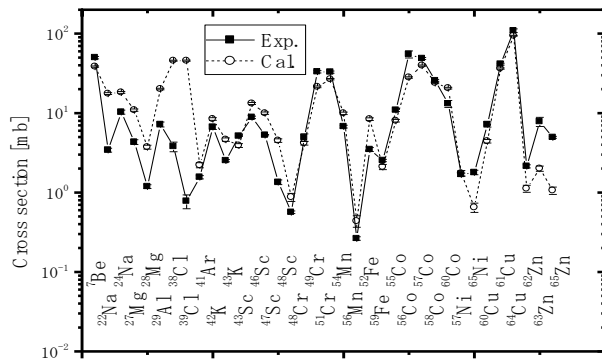
Normalized total neutron yield above 5 meV integrated between 0° and 90° using the equation below from the measured data which is shown by the symbols. The solid lines are from the calculation using the equation below. (Kurosawa et al. at HIMAC, P.R. C in 2000)

$$Y = \frac{1.5 \times 10^{-6}}{N_T^{1/3}} E_P^2 (A_P^{1/3} + A_T^{1/3})^2 N_P \frac{A_P}{Z_P^2},$$

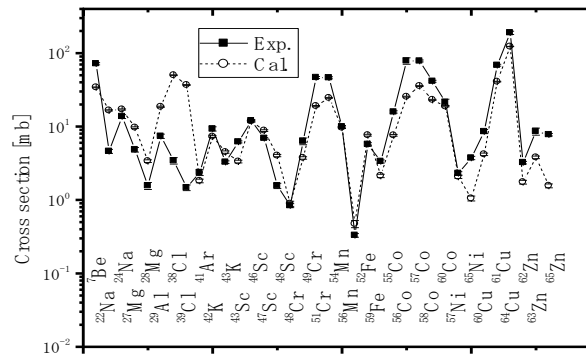
N_T and N_P are the neutron numbers of the target and projectile, A_T and A_P are the mass numbers of the target and projectile, Z_P is the atomic number of the projectile, and E_P is the incident energy per nucleon.

Measured list of spallation product cross sections

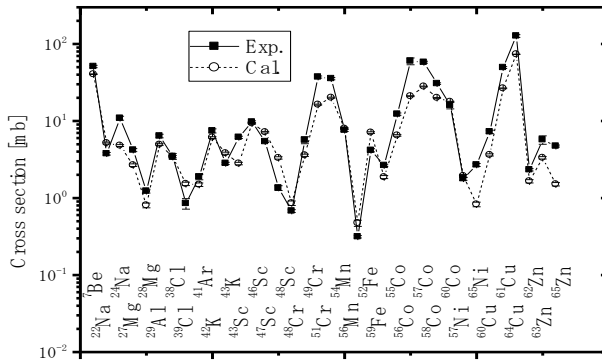
Beam	Energy	Target	Facility	Reference
^{14}N	278 AMeV	$^{\text{nat}}\text{Cu}$	PPA	[22]
^{12}C	2083 AMeV	$^{\text{nat}}\text{Cu}$	Bevalac	[23]
^{40}Ar	2000 AMeV	$^{\text{nat}}\text{Cu}$	Bevalac	[24]
^{12}C	2100 AMeV	$^{\text{nat}}\text{Ag}$	Bevalac	[25]
^{20}Ne	211 AMeV	$^{\text{nat}}\text{Cu}$	Bevalac	[26]
^{20}Ne	377 AMeV	$^{\text{nat}}\text{Cu}$	Bevalac	[26]
^{12}C	135 AMeV	$^{\text{nat}}\text{Cu}$	RIKEN	[27]
^4He	100 AMeV	C, Al, Cr, Fe, Ni, Cu, Pb	HIMAC	[28,29]
^{12}C	100 AMeV	C, Al, Cr, Fe, Ni, Cu, Pb	HIMAC	[28,29]
^{20}Ne	100 AMeV	C, Al, Cr, Fe, Ni, Cu, Pb	HIMAC	[28,29]
^4He	230 AMeV	C, Al, Cr, Fe, Ni, Cu, Pb	HIMAC	[28,29]
^{12}C	230 AMeV	Al, Cr, Fe, Ni, Cu, Pb	HIMAC	[28,29]
^{20}Ne	230 AMeV	C, Al, Cr, Fe, Ni, Cu, Pb	HIMAC	[28,29]
^{40}Ar	230 AMeV	C, Al, Cr, Fe, Ni, Cu, Pb	HIMAC	[28,29]
^{12}C	400 AMeV	C, Al, Cr, Fe, Ni, Cu, Pb	HIMAC	[30]
^{20}Ne	400 AMeV	C, Al, Cr, Fe, Ni, Cu, Pb	HIMAC	[30]
^{40}Ar	400 AMeV	C, Al, Cr, Fe, Ni, Cu, Pb	HIMAC	[30]
^{28}Si	800 AMeV	C, Al, Cr, Fe, Ni, Cu, Pb	HIMAC	[30]
^{12}C	100 AMeV 200 AMeV	$^{\text{nat}}\text{Cu}$, Co ^{63}Cu , ^{65}Cu , Al, Co	GSI TWA-ITEP	[32] [33]
^{40}Ar	500 AMeV, 800 AMeV	Cu	GSI	[32]



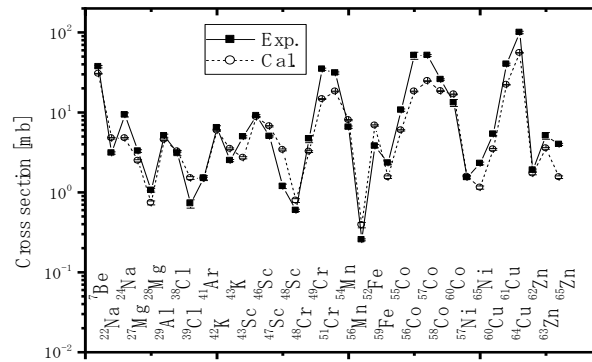
(a) 230 MeV/ nucleon Ar



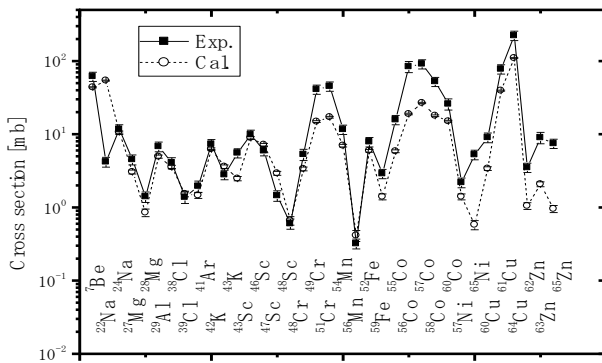
(b) 400 MeV/ nucleon Ar



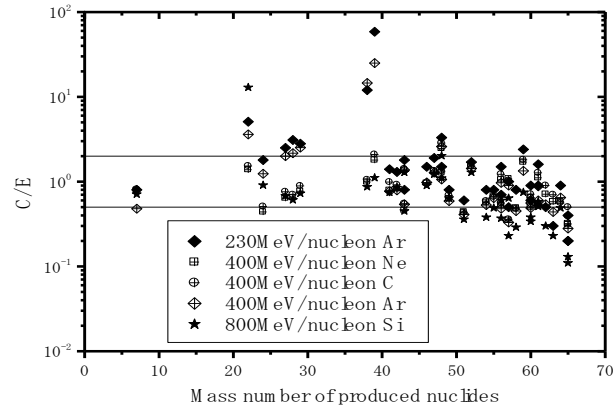
(c) 400 MeV/ nucleon Ne



(d) 400 MeV/ nucleon C



(e) 800 MeV/ nucleon Si



(f) C/ E Value

Comparison of measured reaction cross sections of nuclides produced in Cu for various projectiles with PHITS Monte Carlo calculation by Yashima et al.

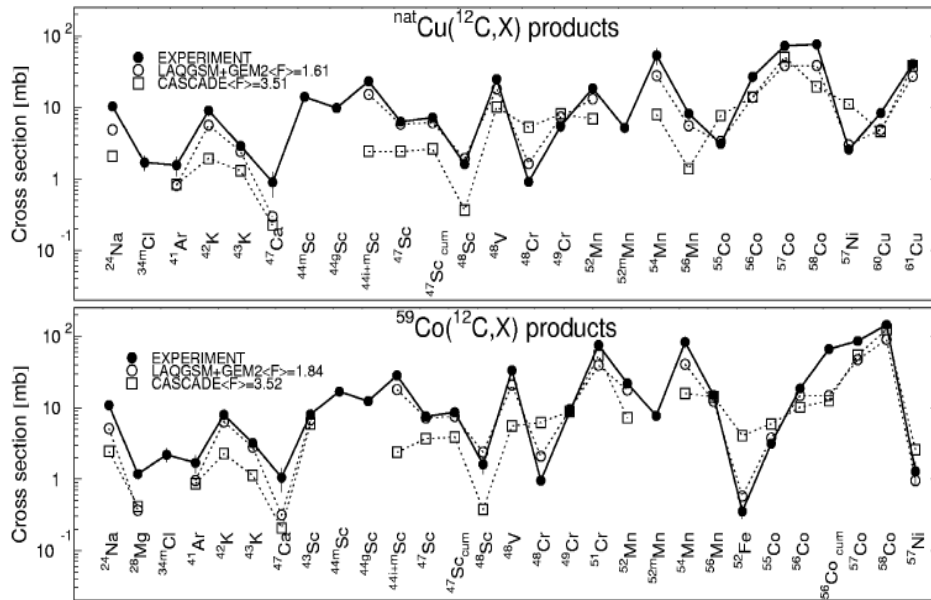
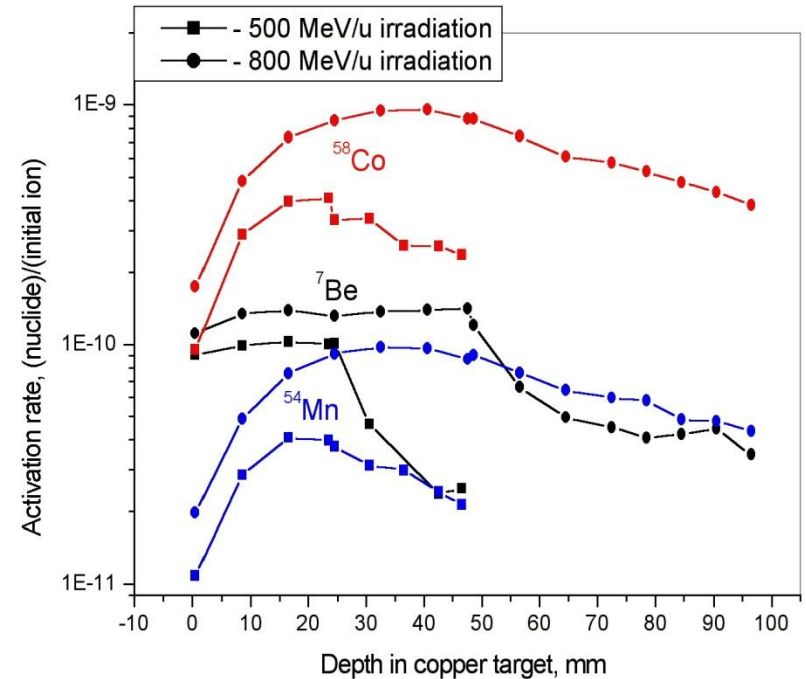


Fig. 4. Detailed comparison between experimental and simulated cross sections of radioactive reaction products in ^{59}Co and ^{nat}Cu induced by $0.2\text{ GeV/u }^{12}\text{C}$. The cumulative cross sections are labeled with a "cum" when the respective independent cross sections are also shown.



Comparison of measured cross sections radioactive reaction products in Co and Cu induced by 200 MeV/nucleon C with the LAQGSM+GEM2 and CASCADE calculations. (Titarenko et al. at TWA-ITEP, 2003)

Spatial distribution of residual activities within Cu target depth for 500 MeV/nucleon and 800 MeV/nucleon Ar ion irradiation. (Fertman et al. at GSI, 2002)
Lighter nuclides are mainly produced by primary particles and heavier nuclides can be also produced by secondary particles with the target depth

Summary

- Heavy ion data have already been published as a book, “Handbook on secondary particle production and transport by high energy heavy ions” by Takashi Nakamura and Lawrence Heilbronn from World Scientific Publ. Co. in 2006.
- For publishing the accelerator shielding handbook, I have written the following three chapters, cooperating with Drs. Heilbronn and Iwase
 - 7. Macroscopic Benchmarking
 - 7.1 Thick target yields
 - 7.2 Shielding experiments
 - 7.5 Heavy ions
 - and one chapter together with Drs. Uwamino, Fehrenbacher and Ronningen
 - 11. Accelerator Specifics
 - 11.4 Heavy ions
- References numbered in tables are all described in these manuscripts.

This review talk is a brief summary of 7.1 and 7.5.